Geological Magazine

www.cambridge.org/geo

A revised chemical weathering and sediment provenance history for the Late Miocene to recent Laxmi Basin, Arabian Sea

Peter D. Clift[1,2,3] and Jacqueline G. Curtis[3]

[1]Department of Earth Sciences, University College London, London WC1E 6BS, UK; [2]Institute of Marine and Environmental Sciences, University of Szczecin, Mickiewicza 16, 70-383 Szczecin, Poland and [3]Department of Geology and Geophysics, Louisiana State University, Baton Rouge, LA 70803, USA

Original Article

Cite this article: Clift PD and Curtis JG. A revised chemical weathering and sediment provenance history for the Late Miocene to recent Laxmi Basin, Arabian Sea. *Geological Magazine* **161**(e20): 1–13. https://doi.org/10.1017/S0016756824000499

Received: 11 August 2024
Revised: 9 October 2024
Accepted: 6 November 2024

Keywords:
Weathering; sediment; geochemistry; provenance; Himalaya

Corresponding author:
Peter D. Clift; Email: peter.clift@ucl.ac.uk

Abstract

Measuring chemical weathering histories in submarine fan deposits is critical if the impact of orogenic erosion on atmospheric CO_2 levels is to be understood, yet existing records are often noisy and hard to interpret. In this study, we selected mudstones from two International Ocean Discovery Program (IODP) sites from the Indus submarine fan and carefully removed the biogenic carbonate. The resulting records of chemical weathering show two trends, one of reducing chemical alteration since ~8 Ma and which is associated with the Indus River, while a second trend is linked to sediment delivery from peninsular India. The second trend shows little temporal variation. Sediment deposited at IODP Site U1456 in the central Laxmi Basin is preferentially, but not exclusively, Indus-derived, while that at Site U1457 on the eastern flank of Laxmi Ridge is more peninsula-derived. Both trends show much less variability than seen in earlier studies in which various grain-size fractions were integrated together. The efficiency with which CO_2 is removed from the atmosphere during chemical weathering has decreased over time in the Indus River-derived material. This reflects both lower degrees of alteration in the sediment since the late Miocene and increasing derivation of sediment from Himalayan sources, rather than more mafic Karakoram-Kohistan rocks. Previous estimates of CO_2 consumption have overestimated the contribution that the Indus Basin has made to reducing atmospheric CO_2 by ~28–68%. This work emphasizes the importance of analysing appropriate largely silt-sized sediment when considering submarine fan records and in rigorously removing biogenic carbonate.

1. Introduction

The process of chemical weathering of silicate minerals forms a critical part of the Earth's carbon cycle because the atmospheric greenhouse gas CO_2 is consumed during their breakdown and the subsequent fixture of carbon into carbonate sediment in the ocean. Once deposited in this way, carbon can be stored over long periods of geologic time (Berner & Berner 1997; Kump & Arthur 1997) and even returned to the mantle (Kelemen & Manning 2015; Clift 2017). In order to estimate how much CO_2 is being consumed, it is important to know not only the volumes of material involved but also the change in the major element chemistry of the degraded sediment compared to its original fresh bedrock composition (France-Lanord & Derry 1997; Clift & Jonell 2021). However, an accurate estimate of both sediment and source rock chemistry can be difficult to ascertain. In this study, we examine potential uncertainties in the composition of the weathering products (i.e. the sediment) and in particular look at the Indus submarine fan of the western Indian Ocean (Fig. 1A), which is the primary repository for sediments eroded from the Western Himalaya and Karakoram (Naini & Kolla 1982; Droz & Bellaiche 1991; Clift *et al.* 2001).

The Indus Fan is the second largest sediment body in the world, falling only slightly behind its Eastern neighbour, the Bengal Fan, located in the Bay of Bengal. The Indus Fan's impressive size (4.5×10^6 km^3) is owed to the uplift and erosion of the Himalayas, which has for many years been invoked as one of the primary controls over global weathering fluxes and in turn on atmosphere CO_2 concentrations (Raymo & Ruddiman 1992). However, a recent compilation by Clift *et al.* (2024b) argues differently. Using published geochemical data (Zhou *et al.* 2021) in the aftermath of a campaign of scientific drilling conducted by the International Ocean Discovery Program (IODP) in the Asian marginal seas, the team was able to estimate how much CO_2 was consumed during the Neogene by the major drainage systems of south and southeast Asia. That work argued that the Himalayas have not dominated the global carbon budget, except potentially since 2–3 Ma, when an increasing weathering flux contributed to the intensification of cooling linked to northern hemisphere glaciation (NHG)(Clift *et al.* 2024b). If this assessment is correct, then other parts of the world may be contributing to an enhanced weathering flux

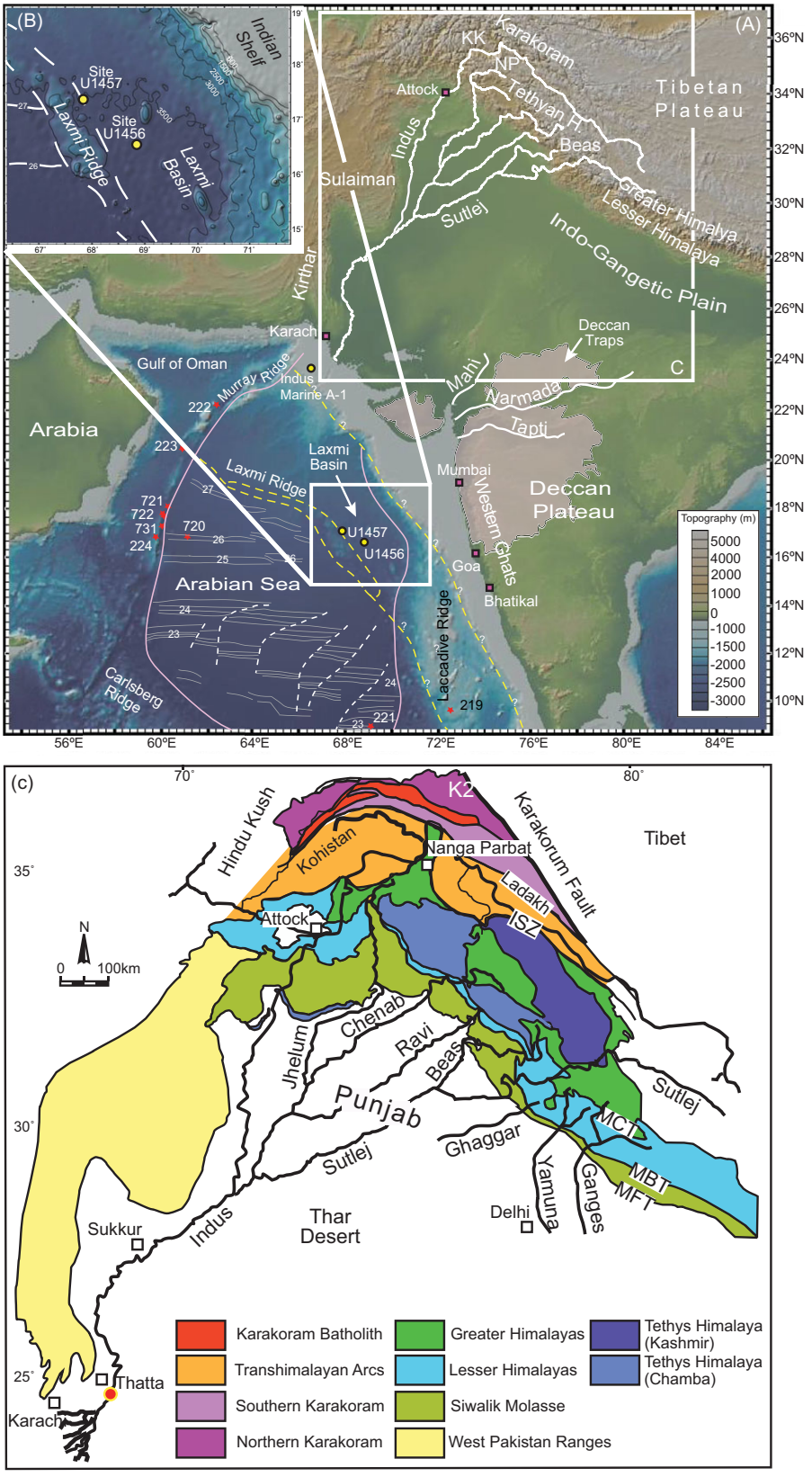

Figure 1. (A) Shaded bathymetric and topographic map of the Arabian Sea area showing the locations of the drilling sites within the Laxmi Basin, considered by this study. The map also shows the primary source terranes and the major tributary systems of the Indus River, as well as smaller peninsular Indian rivers (white lines) that may have provided material to the drill sites. (B) The inset map shows details of the Laxmi Basin and the locations of the drill sites considered in this study. Magnetic anomalies are from Miles *et al.* (1998). White dashed lines show transform faults. NP = Nanga Parbat. (C) Geological map of the Western Himalaya showing the major tectonic units that are eroded by the Indus River and its tributaries. Major rivers are shown as solid black lines. The map is modified after Garzanti *et al.* (2005). Rivers are shown in thick black lines. ISZ = Indus Suture Zone; MCT = Main Central Thrust; MBT = Main Boundary Thrust and MFT = Main Frontal Thrust.

(Bayon *et al.* 2023; Martin *et al.* 2023; Clift *et al.* 2024a), but in all cases, any quantitative estimate critically depends both on accurate determination of the sediment volumes and also their chemical composition.

Several important uncertainties still exist that inhibit the construction of accurate regional weathering and carbon budgets. A recent study showed that the estimated efficiency of CO_2 consumption in sediments from the Bengal Fan was critically

https://doi.org/10.1017/S0016756824000499 Published online by Cambridge University Press

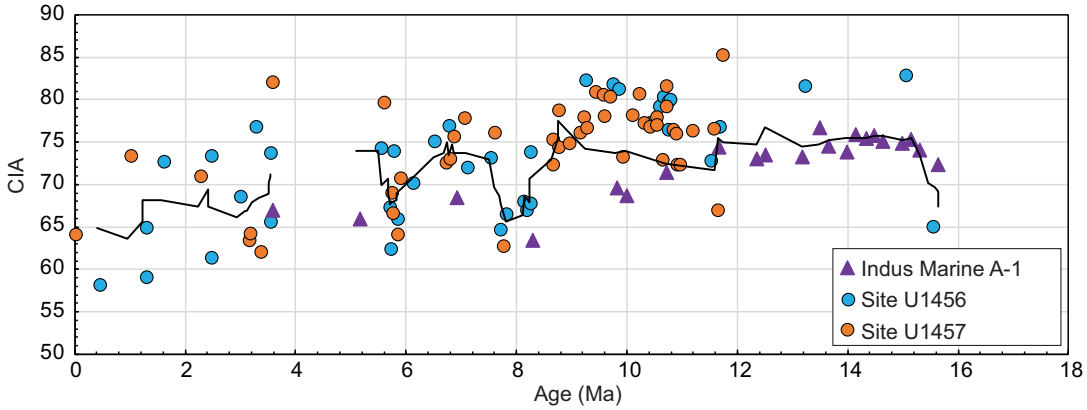

Figure 2. Plot of evolving Chemical Index of Alteration (CIA) at Sites U1456 and U1457, as well as Indus Marine A-1 from Zhou *et al*. (2021). The black line is a five-point running average. The trend is towards lower values, but there is a lot of scatter.

dependent on them being rigorously decarbonated (Tachambalath *et al.* 2023). Because calcium (together with Na, K and Mg) is an important element used in calculating the amount of CO_2 consumed per unit volume of sediment (France-Lanord & Derry 1997), it is essential that sediment analysed for this purpose has all of its biogenic carbonate removed prior to analysis. More recent studies often omit the decarbonization process or fail to fully decarbonate their samples, making it difficult to integrate older data into regional syntheses.

Chemical analyses of Indus Fan sediments published by Zhou *et al.* (2021) demonstrate some of the potential complexities. Figure 2 shows the temporal trend in the Chemical Index of Alteration (CIA) (Nesbitt *et al.* 1980) at IODP Sites U1456 and U1457 reconstructed by *Zhou et al.* (2021). CIA is a common proxy for the degree of alteration in sediments (Nesbitt & Young 1982). These data were used to argue for a decrease in the intensity of chemical weathering starting ~8 Ma and that continued to the present day, correlating with decreasing global temperatures at the same time (Westerhold *et al.* 2020). However, the reconstructed trend is noisy, and even the five-point running average employed by the study shows a rather erratic decrease in the value of CIA through time (Fig. 2). This trend contrasts with the regular and smooth decrease in CIA seen in the hemipelagic sediment at Ocean Drilling Program (ODP) Site 1146 in the South China Sea (Clift & Jonell 2021). Is there something intrinsically noisy about environmental records stored in submarine fan complexes, potentially driven by recycling and the wide range of grain sizes, or could this noisy record be a reflection of sampling and sample processing?

Two potential complexities may be causing the poor quality of this submarine fan record. One is whether the decarbonation process was done sufficiently well, while the other questions the potential role of grain size. In general, fine-grained sediments are more altered than coarser material because small grains have a higher surface area to volume ratio, which allows the silicate material to be broken down more rapidly (He *et al.* 2015). A lack of sand in the dominantly silt-clay sediments from ODP Site 1146 in the South China Sea may be one of the reasons that this reconstruction is much less noisy than that found in the Arabian Sea. In contrast, the Zhou *et al.* (2021) study was done with samples taken at regular depth intervals within the Indus Fan, but without any systematic selection for certain size fractions. This is even though the vast majority of the volume of large submarine fans comprises silt-sized material (Stow *et al.* 1985; Bouma 2001). Sand is also present in the fan but is more common in channel and proximal levee complexes. These are volumetrically small compared to the overall stratigraphic architecture, despite being more common in proximal settings (McHargue & Webb 1986; Kolla & Coumes 1991).

Consequently, in this study, we preferentially resampled muddy sediments from IODP Sites U1456 and U1457 (Pandey *et al.* 2016a; Pandey *et al.* 2016b) in order to test whether grain size or carbonate removal may have affected the reconstruction of chemical weathering and in turn influenced estimates of the amount of atmosphere CO_2 removed during the erosion and weathering of the Western Himalaya and Karakoram.

2. Geologic setting

IODP Sites U1456 and U1457 recovered sediments from the Laxmi Basin in the eastern part of the Arabian Sea (Pandey *et al.* 2016a; Pandey *et al.* 2016b). This basin is located immediately adjacent to the passive margin of Western India, offshore the Western Ghats (Fig. 1). The Laxmi Basin is separated from the main Arabian Basin by the Laxmi Ridge (Fig. 1), interpreted as a fragment of continental crust that rifted away from the western Indian margin prior to a jump in the locus of extension and the onset of sustained seafloor spreading to the west of Laxmi Ridge (Talwani & Reif 1998; Pandey *et al.* 2020). In general, the sediment in the Laxmi Basin has been interpreted to be mostly derived by supply from the Indus River, located to the north (Clift *et al.* 2019; Andò *et al.* 2020; Zhou *et al.* 2022), although there is evidence for some sediment supply from the east, from the passive margin of the Indian peninsula (Yu *et al.* 2019; Cai *et al.* 2020; Carter *et al.* 2020; Garzanti *et al.* 2020). The drilled fan sequence is a continuous succession of hemipelagic muds and graded silty-sand turbidites and was truncated by a major mass wasting complex (MWC) emplaced just prior to 10.8 Ma (Dailey *et al.* 2019). The fan section pre-dating the MWC has been removed by erosion at Site U1457, while drilling recovered only a short sequence under the MWC at Site U1456 dated at ~15 Ma (Routledge *et al.* 2020).

The sediments analysed here were taken from sequences dominated by mudstones, but with interbedded silt and sand layers that were preferentially avoided (Fig. 3). Most of the sediments are hemipelagic, but the coarser-grained material is often graded and is interpreted to have been deposited from turbidity currents either on lobes or within channels of the submarine fan (Andò *et al.* 2020). Sediment from Site U1456 is sandier than that at Site U1457, especially in Upper Pliocene and Lower Pleistocene sediments

https://doi.org/10.1017/S0016756824000499 Published online by Cambridge University Press

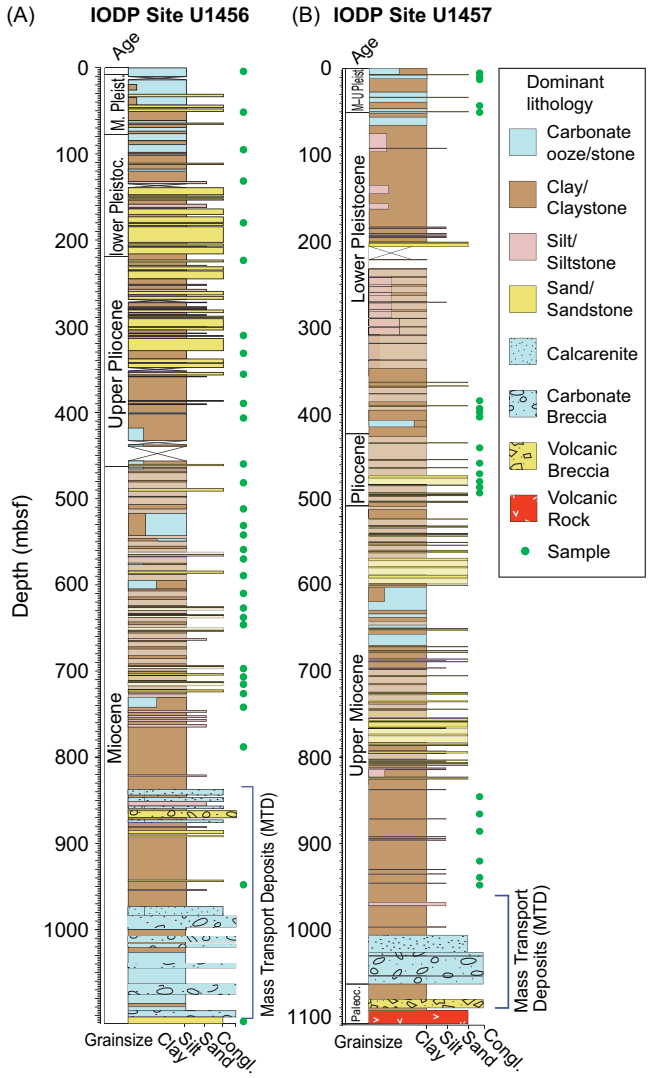

Figure 3. Simplified lithologic logs of the two drill sites considered in this study. (A) International Ocean Discovery Program (IODP) Site U1456, (B) IODP Site U1457. Modified from Pandey *et al.* (2016c). Congl. = conglomerate.

(Fig. 3). There are significant sections where the sediment is uniformly muddy in character, but there are also carbonate or carbonate-rich mudstone layers, testifying to episodes of pelagic sedimentation and abandonment of the fan, at least locally. The biostratigraphic-magnetostratigraphic framework indicates that there are significant time gaps (disconformities) within the sequence above that are associated with the MWC (Routledge *et al.* 2020). These disconformities are interpreted to reflect the avulsion of the primary depositional lobe both within Laxmi Basin and away from Laxmi Basin and into the main part of the Arabian Basin, west of Laxmi Ridge.

Zircon U-Pb and apatite fission track dating of sandy materials also indicate that most of the coarse-grained sediment has been supplied from the Indus River (Zhou *et al.* 2020; Zhou *et al.* 2022), but the origin of the fine-grained material has been disputed. Upper Miocene sediments from Site U1457 yielded pollen and biomarkers that were indicative of some of the sediment coming directly from peninsular India (Feakins *et al.* 2020). Likewise, in the younger part of the drilled section, studies have argued for alternating supplies from the peninsula and from the delta (Cai *et al.* 2019; Clift *et al.* 2019; Carter *et al.* 2020; Garzanti *et al.* 2020). Resolving these contrasting supplies is not entirely straightforward because many of the proxies used offer non-unique solutions.

During the 10.8 Ma of sedimentation recorded at the drill sites since the MWC, the source of the sediments has seen a progressive evolution towards more Himalayan supply as the focus of erosion within the Indus Basin and shifted away from sediment derived from the Karakoram (Clift *et al.* 2019; Zhou *et al.* 2022). In particular, the uplift of the Lesser Himalaya impacted the supply of sediment to the Arabian Sea by increasing the amount coming from the radiogenic ancient Indian continental crust (Najman *et al.* 2009; Exnicios *et al.* 2022) versus the more primitive rocks of the Karakoram. The latter were more dominant before ~8 Ma. Zhou *et al.* (2022) used detrital zircon U-Pb age data combined with numerical unmixing methods (Sundell & Saylor 2017) to estimate that around 70% of the sand reaching the drill sites before 8 Ma was from the Karakoram but that this had fallen to ~35% by 5.7 Ma. Associated bulk sediment Nd isotope analysis was consistent with this estimate and supported a progressive increase in flux from the Lesser Himalaya from 5.7 Ma until the present day (Clift *et al.* 2019).

The change in the provenance of the Indus River is important for chemical weathering records because the sediments eroded from the Himalayas have bedrock compositions that are more consistent with average upper continental crust (UCC) (Hodges 2000), while those derived from the Karakoram or Kohistan have more primitive, mafic compositions (Searle *et al.* 1989; Khan *et al.* 1997; Jagoutz *et al.* 2007). Because the amount of CO_2 consumed during chemical weathering is controlled by the difference between the sediment composition and the original bedrock, alteration of reactive Ca–Mg-bearing mafic rocks, such as those exposed in the Karakoram-Kohistan, typically results in higher degrees of atmospheric CO_2 consumption (Caves Rugenstein *et al.* 2019). It is this compositional difference between the source rocks of the sediments of the Arabian Sea that makes them more effective in sequestering CO_2 from the atmosphere than the sediments of the Bengal Fan (Clift & Jonell 2021; Clift *et al.* 2024b).

3. Sampling

Fifty-two samples were selected from both Sites U1456 and U1457 to assess whether earlier work was biased by grain-size issues and/or incomplete decarbonation. Thirty-one samples were taken from Site U1456 and 21 from Site U1457. Site U1456 was favoured because of its location in the central part of the Laxmi Basin where it is more likely to be the recipient of sediment transported from the Indus Delta to the north, whereas Site U1457 is located on the flanks of the Laxmi Ridge and could be less strongly Indus River influenced. In this work, we specifically targeted fine-grained lithologies, typically described as various types of mudstones (silt-clay mixtures) by the shipboard core descriptions (Pandey *et al.* 2016a; Pandey *et al.* 2016b). We attempted to achieve the best temporal control as possible by employing the revised age models from Routledge *et al.* (2020). All samples were analysed for grain size and decarbonated sediment chemistry.

4. Methodology

4. a. Grain-size analysis

A total of 52 samples from Sites U1456 and U1457 had their grain size determined following the procedure of Hülse & Bentley

https://doi.org/10.1017/S0016756824000499 Published online by Cambridge University Press

(2012). About 2 g of sample were placed in a 50 ml plastic centrifuge tube with 5.75 ml of $NaPO_3$ solution. Each tube was capped and vortexed to deflocculate clay-sized sediment and separate organic particles. The sample was poured through an 850 µm sieve to help remove large particles of organic matter. The polypropylene tube was placed into a centrifuge to settle the sediment at the bottom of the vial. The vials were then run at ~25 rotations per minute for 60 minutes, and the supernatant was then removed. About 2 ml of $NaPO_3$ was then added to the centrifuged sample, as well as 5 ml of H_2O_2. Small amounts of acetone were sprayed in the vials to stabilize the reaction, following which the samples were placed in a hot bath set at 70°C overnight. Once removed from the hot bath, the supernatant was removed from the vials, and the samples were transferred into plastic tubes with caps to be vortexed for analysis. The samples were then analysed using a Beckman-Coulter (LS 13-320SW Laser Diffraction Particle Size Analyzer Single Wavelength) at Louisiana State University (LSU). Results, including full grain-size spectra up to 282 µm, mean, median, kurtosis and skewness, are shown in Table S1.

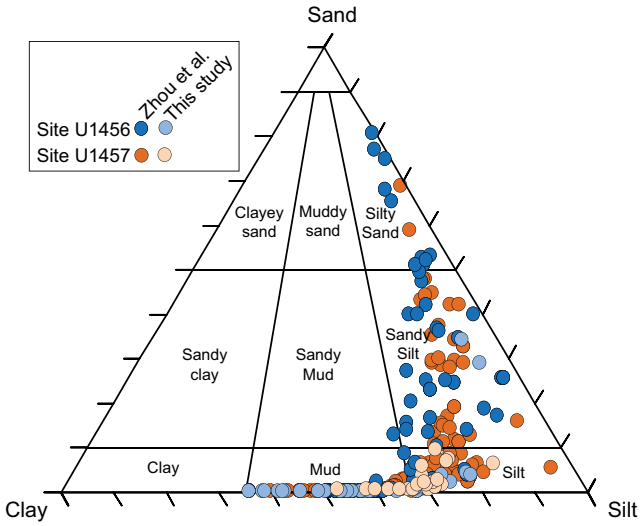

Figure 4. Grain-size range of all samples analysed for U-Pb zircon dating from the Laxmi Basin is shown on the scheme of Folk (1974). Previously published data is from Zhou *et al.* (2021).

4. b. Major and trace element analysis

Sediments were decarbonated with 20% acetic acid for at least two days until no further bubbles were noted, then washed with distilled and deionized water with a purity of 9–12 megaohms and hand powdered. Decarbonated powder samples for major element geochemistry were processed and analysed in the Chevron Geomaterials Characterization Laboratory (CGCL) in the Department of Geology and Geophysics at LSU. The samples were ground in a mortar and pestle and then transferred into a hardened steel vial to be milled to a grain size of <30 µm using a SPEX® SamplePrep 8000M mixer/mill. Approximately 4.00 ± 0.04g of powder from each sample and 1.00 ± 0.01g of SPEX® SamplePrep UltraBind® powder was weighed and mixed using the 8000M mixer/mill. The mixture was then pressed into a pellet using a bench top 20 tonne hydraulic pellet press and a 31 mm pellet die.

Analysis was carried out using the Bruker S2-PUMA energy-dispersive X-ray fluorescence (XRF) instrument in the CGCL. All analyses were performed under a vacuum using a Pd X-ray source. An accelerating voltage and current of 20 kV and 0.25 µA with no primary filter were used for Na_2O, MgO, Al_2O_3, SiO_2 and P_2O_5, while 40 kV and 0.5 µA and a 0.5 mm Al filter was used for K_2O, CaO, TiO_2, MnO and Fe_2O_3, as well as the remaining trace elements. The analyses were calibrated using 19 international standard reference materials, including AGV-2, BIR-1a, G-2, GSP-2, RGM-1, SDC-1 and W-2 from the United States Geological Survey (USGS); JA-3, JB-2, JB-3, JG-2, JG-3, JR-1 and JP-1 from the Geophysical Survey of Japan (GSJ); and BCS-309, BCS-313-2, BCS-375, BCS-376/1 and BCS-388 from British Chemical Standard. Replicate analysis (N = 10) of the USGS SGR-1b and GSJ JB-3, JA-3, JSd-1 and JLk-1 standards was performed to check for drift and assess the quality of the calibration prior to analysis. Secondary standards (e.g. JA-3, SCo-1) were analysed during every analytical run to monitor for instrumental drift and assess the continued quality of the calibration. Concentrations of Na_2O, MgO, Al_2O_3, SiO_2, P_2O_5, K_2O, CaO, TiO_2, MnO and Fe_2O_3, as well as the loss on ignition, are shown in Table S2. CIA (Nesbitt *et al.* 1980) is calculated using the following molar equation.

$$CIA = (AIO/AIO + CaO* + NaO + KO) \times 100$$

5. Results

Grain-size analysis reveals that the sediments selected were largely successful in sampling only fine-grained material. Figure 4 shows the triangular diagram from Folk (1974). Most of the sediments considered here are defined as mud or silt under this scheme, although two samples from Site U1456 were defined as sandy silt. This represents true siliciclastic sandy silt and is not the product of carbonate shells being present. It is noteworthy that the sediments from Site U1456 are mostly finer grained than those from Site U1457, which tend to plot more in the silt field. When compared with the sediments analysed in the earlier Zhou *et al.* (2021) study, we note that many of their analyses were made on sandy-silts or silty-sand material, consistently coarser grained than the material examined here.

Decarbonated sediment major element chemistry reflects not only the source bedrock composition but also the influence of sediment transport on the material being analysed. In the discrimination diagram of Singh *et al.* (2005), our samples plot towards the lower left of the diagram (Fig. 5A), away from the UCC average (Rudnick & Gao 2003) and implying preferential enrichment in quartz, with associated relative loss of material such as biotite, muscovite and clay. The fact that many of these sediments are quite fine grained makes this a little surprising, although it emphasizes the importance of quartz-dominated silt in the make-up of these materials. Enrichment in quartz reflects the breakdown of chemically unstable phases, such as the micas and the concentration of quartz by hydrodynamics sorting. We note that the sediments in this study show this effect even more than the sediments in the Zhou *et al.* (2021) work, although there is significant overlap.

The concentrations of some water-immobile elements are closely tied to certain minerals and thus to provenance. These potentially act as tracers that might quantify the competing influence of the Indus River and peninsular India. The latter is dominated by the Deccan Traps in the immediate onshore region,

https://doi.org/10.1017/S0016756824000499 Published online by Cambridge University Press

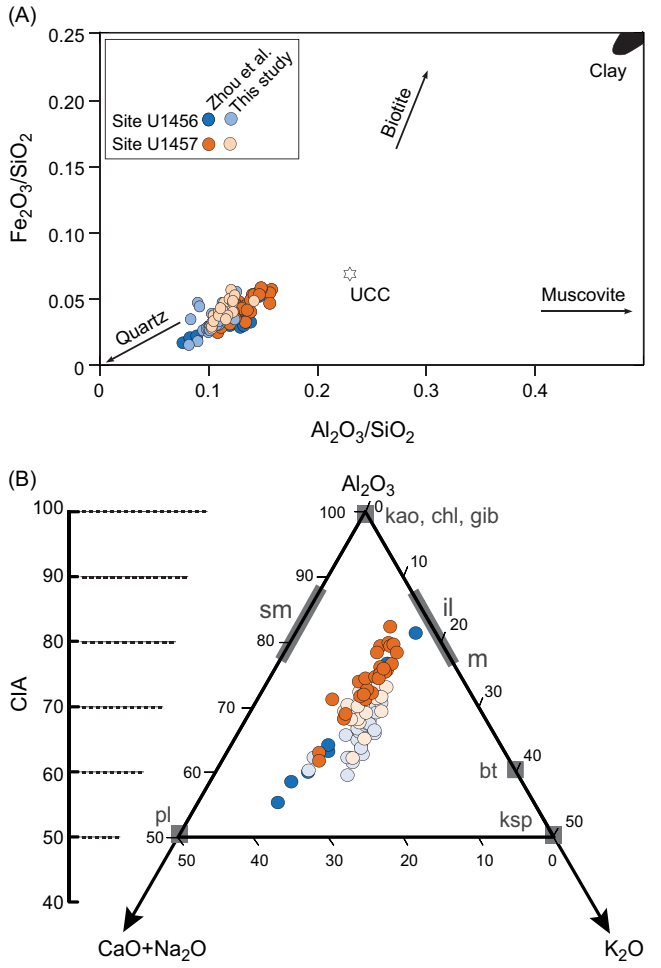

Figure 5. (A) Plot of Al_2O_3/SiO_2 versus Fe_2O_3/SiO_2 after Singh *et al.* (2005). Lower ratios indicate an increase in the quartz proportion and a depletion of phyllosilicates. The linear trend corresponds to the mineralogical sorting of these sediments during fluvial transport. The star corresponds to the average Upper Continental Crust (UCC) (Taylor & McLennan 1995). (B) Geochemical signature of the analysed samples illustrated by a (CaO* + Na_2O-K_2O-Al_2O_3) CN-K-A ternary diagram (Fedo *et al.* 1995). CaO* represents the CaO associated with silicate, excluding all the carbonate. Samples closer to A are rich in kaolinite, chlorite and/or gibbsite (represented by kao, chl and gib). Chemical Index of Alteration (CIA) values are also calculated and shown on the left side, with its values correlated with the CN-K-A. Samples from the delta have the lowest values of CIA and indicate high contents of CaO* and Na_2O and plagioclase. Abbreviations: sm (smectite), pl (plagioclase), ksp (K-feldspar), il (illite), m (muscovite), bt (biotite).

as drained by the Narmada, Tapti and Mahi rivers (Fig. 1). Zr concentration is largely a reflection of zircon abundance. This mineral is most common in felsic igneous rocks and in siliciclastic sedimentary rocks but is less common in mafic rocks. Zr concentrations might be expected to rise with greater erosion from older continental (i.e. Himalayan or Indian cratonic) rocks. There is a weakly defined trend to higher Zr concentrations through time at both sites, rising from ~130 ppm at 10 Ma to ~160 ppm in recent times (Fig. 6B). This trend is not linked to grain size as mean grain size and Zr concentrations show an $R^2 = 0.16$ correlation. Ti is concentrated in rutile and ilmenite grains, which are found in high-grade metamorphic rocks and intrusive igneous rocks (Zack & Kooijman 2017). Ti abundances in fine-grained sediments are also strongly controlled by the presence of clays, but there is no correlation between TiO_2 and mean grain size in this dataset ($R^2 = 0.001$). Ilmenite is especially associated with cumulate igneous intrusions (Anthony *et al.* 2022), although it is not exclusive to felsic or mafic rocks. The concentrations of Ti do not change much over time, although sediments from Site U1456 have lower average contents (0.97%) compared to those at Site U1457 (1.24%) (Fig. 6A).

Cr is primarily found in chromite, which in turn is associated with mafic and ultramafic intrusions (Dawson & Smith 1975; Lorand & Ceuleneer 1989), so its abundance might be associated with erosion of ophiolite and/or arc lower crustal rocks, such as found in the Karakoram, Kohistan or in the ophiolites in the Indus Suture Zone. However, Cr contents in the Laxmi Basin sediments show no significant temporal evolution (Fig. 6C). None of these stable element provenance proxies correlate very much with the Nd isotope record from the sites. Nd is generally considered to be a good provenance proxy linked to the age of the source rocks and is not affected by chemical weathering (Goldstein *et al.* 1984). Earlier Nd isotope work featured a cluster of high ε_{Nd} value samples, which were associated with run-off from the Indian peninsula (Fig. 6D), as well as a trend to decreasing values linked sediment supply from the Indus River and reflecting greater degrees of Himalayan erosion through time (Clift *et al.* 2019).

6. Discussion

The state of chemical weathering of the sediments considered here can be assessed in the (CaO* + Na_2O), K_2O and Al_2O_3 (CN-K-A) triangular diagram of Fedo *et al.* (1995), where CaO* represents the CaO associated with silicate (Fig. 5B). In this plot, freshly eroded continental material typically lies at the bottom of the triangle, while progressive chemical weathering displaces the composition towards the top as water-mobile components are removed and Al_2O_3 is correspondingly relatively enriched. The sediments considered in this work form part of an array stretching from the bottom left-hand corner towards the mid-right-hand side of the triangle, towards an illite and mica end member. This is caused by the breakdown of the original rock fragments into clay minerals.

The new data are largely consistent with those in the earlier study (Zhou *et al.* 2021), although they tend to plot a little below the previously analysed material, implying less chemical weathering than previously measured. This is despite the material being mostly finer grained than that considered before. The reduced range of compositions on this plot reflects the more limited grain size considered in this study. The same plot allows the degree of weathering to be assessed according to the CIA proxy. Samples from Site U1456 have slightly lower CIA values, a minimum of ~59, while Site U1457 samples have higher values, up to a maximum of 73.

6. a. Grain size and alteration

We investigate how the grain size of the sediment may be linked to its degree of chemical alteration. Considering the full range of grain sizes analysed by Zhou *et al.* (2021), it is possible to see that there is a rough correlation whereby sediments with the largest grain size (lowest φ values) generally have the lowest CIA values (Fig. 7A), whereas the finest grained sediments (highest φ values) have the highest CIA values. This is consistent with the idea of the fine-grained material being more altered than the coarse grained. However, if we only consider the dataset generated in this study, then we see that no clear relationship is apparent (Fig. 7B). The highest CIA values are not present in our dataset. Overall, the material from Site U1457 is coarser grained than that found at Site

https://doi.org/10.1017/S0016756824000499 Published online by Cambridge University Press

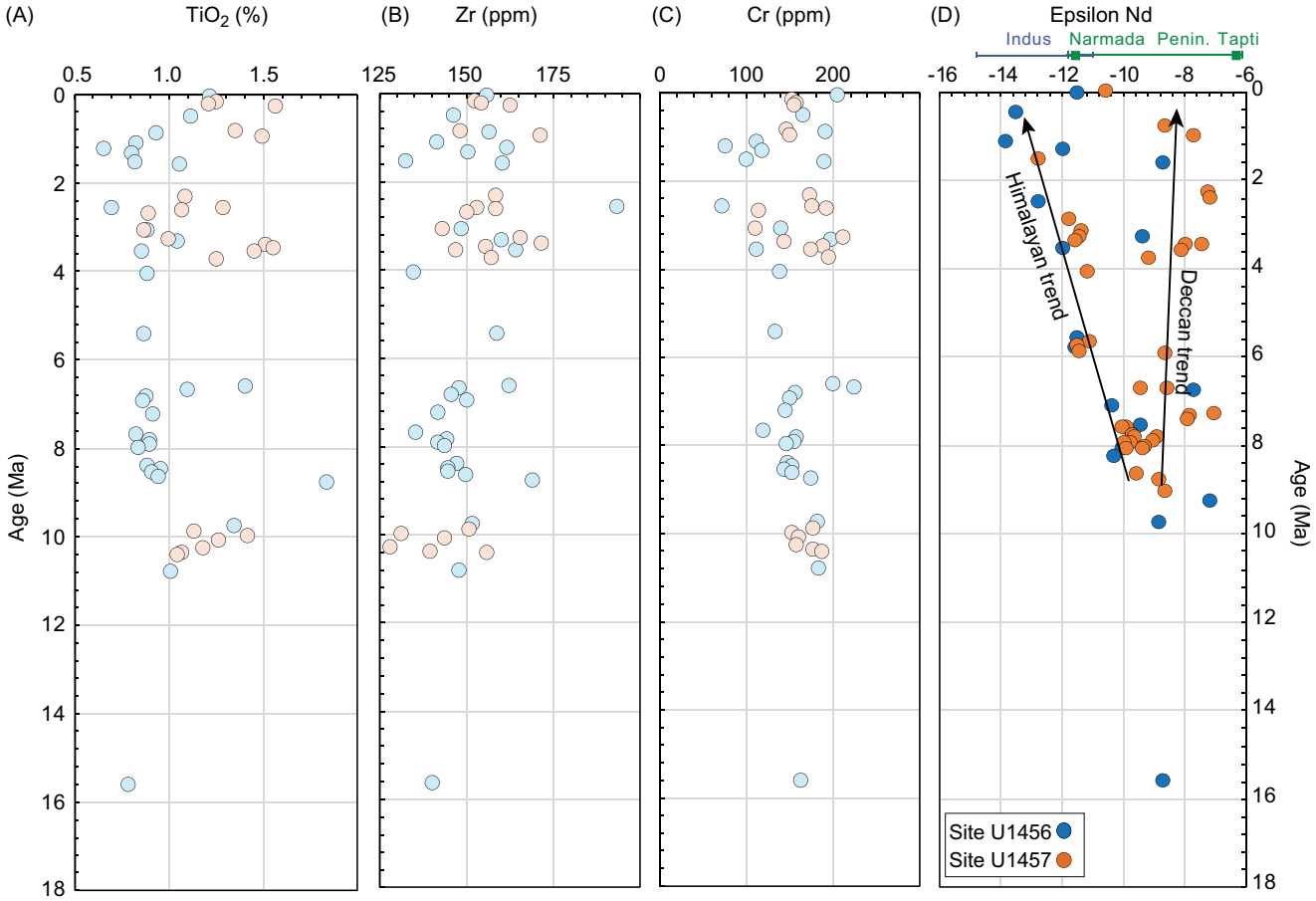

Figure 6. Temporal evolution in (A) Ti_2O, (B) Zr and (C) Cr contents. (D) Nd isotope data from Clift *et al.* (2019) are also shown for comparison. Note the two trends that develop after ~8 Ma showing falling values towards the Last Glacial Maximum to recent range and a more constant trend towards the range of Indian peninsula rivers (Kessarkar *et al.* 2003). Green squares represent modern compositions of the peninsula-draining Narmada and Tapti rivers. Penin = Peninsular.

U1456, but the Site U1457 sediment has higher average CIA values (70.6 vs 68.0), the opposite of what was observed in the previous study. Although this may seem counter-intuitive, this may point to the material at Site U1457 being preferentially derived from a more weathered area than that sourcing Site U1456. Furthermore, within each site, it is possible that there is insufficient grain size variability to make much difference to the alteration state.

6. b. Evolution in weathering

We now investigate whether the new dataset provides a more coherent long-term evolution in chemical weathering trends. The long-term trend in CIA (Fig. 8A) is much better defined than observed in the previous study (Fig. 2) (Zhou *et al.* 2021). During the Pleistocene (<2.58 Ma), our new data indicate CIA averaging 61.8 with a standard deviation (SD) of 2.5; in contrast, the Zhou *et al.* (2021) study estimated CIA averaging 67.6 and with an SD of 5.4. During the Pliocene (2.58–5.3 Ma), CIA values are 69.0 with an SD of 2.1, while Zhou *et al.* (2021) estimate the average CIA at 70.9 with SD of 6.9. Late Miocene (5.3–11.6 Ma) CIA values are 71.5 with an SD of 3.4, while Zhou *et al.* (2021) estimate CIA averaging 72.8 with an SD of 5.3.

At 10 Ma, CIA was ~75, but this falls to values ~65 with a lot of variability by the present day.

It is possible that the strong recent variability may be linked to high amplitude climatic cycles following the onset of NHG. Rates of weathering are dependent on temperature and humidity (West *et al.* 2005). We also note that the highest CIA values in the last 4 Ma are almost exclusively found at Site U1457.

If we consider the alternative proxy CIX (Garzanti *et al.* 2014), which is calculated in the same way as CIA except excluding Ca, then there is a more clear-cut difference between the two sites. Material from Site U1456 shows a trend from values ~77 at 10 Ma, falling to ~68 in recent times. In contrast, the material from Site U1457 maintains a relatively constant CIX value after 10 Ma (Fig. 8B). In both cases, it is possible to compare these values with recent measurements from the Holocene Indus River and its continental shelf (Limmer *et al.* 2012), as well as rivers draining the Indian peninsula (Kurian *et al.* 2013). As might be expected, alteration of sediment in the Indus River drainage is weaker than that seen in the Indian peninsula, reflecting faster erosion driven by active rock uplift and thus little time for weathering in the Himalayan source region. In general, there is a tendency of the Site U1457 material to trend towards peninsular values, while the data from Site U1456 mostly coincide with recent values from the Indus River.

We also examine the degree of chemical alteration using two widely applied proxies involving the ratio of water-mobile alkali elements versus immobile Al. Figure 8C shows that values in K/Al at Site U1456 mostly increase from 10 Ma, when values were ~0.27, and reached ~0.3 in recent geological time. In contrast, a second trend can be seen, dominated by material from Site U1457, which

https://doi.org/10.1017/S0016756824000499 Published online by Cambridge University Press

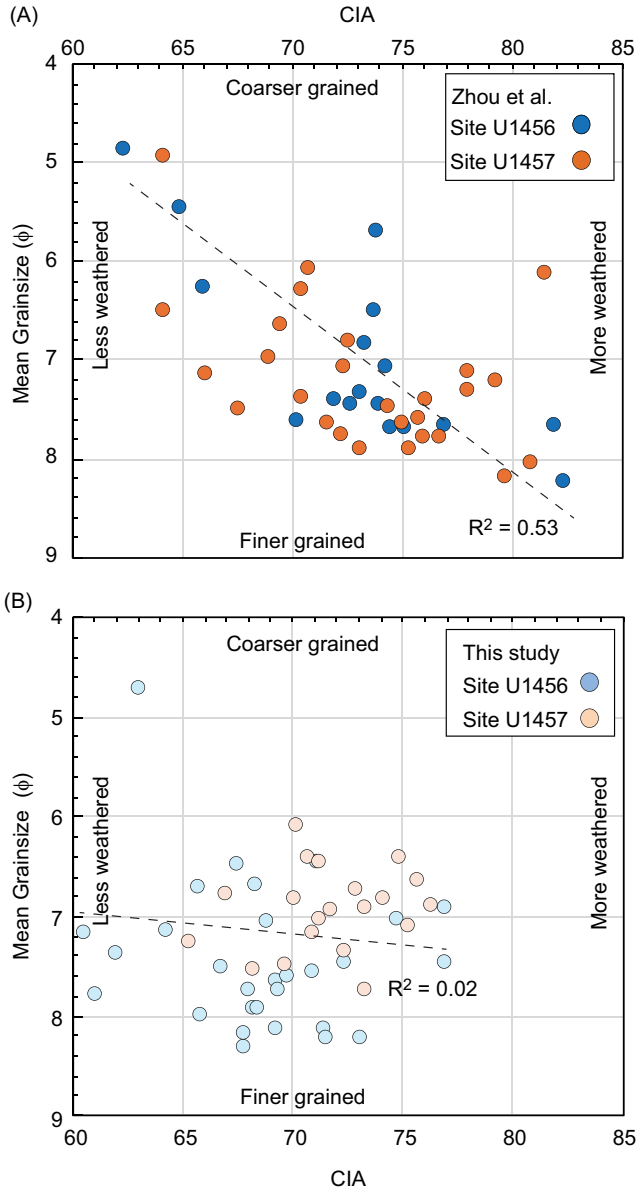

Figure 7. (A) Plot of Chemical Index of Alteration (CIA) versus mean grain size with data from Zhou *et al.* (2021). (B) With data from this study.

started at the same value at 10 Ma but instead slightly decreased to ~0.2 at the present. A very similar arrangement can be seen with Na/Al (Fig. 8D), which on average increases to the present day at Site U1456, indicative of less chemical weathering through time, as predicted by Zhou *et al.* (2021), but again with the most weathered material being preferentially found at Site U1457.

In order to assess whether there might be a relationship between the extent of chemical weathering and the source of sediments, we plot the CIA against the Nd isotope character (ε_{Nd}). Figure 9A shows that there is a positive correlation between Nd isotopic composition, which is entirely determined by sediment provenance (Goldstein *et al.* 1984), and the extent of chemical weathering at both drilling sites, although the correlation coefficient is low ($R^2 = 0.15$ at Site U1456 and 0.11 at Site U1457). This implies that more weathered sediment is preferentially derived from younger more primitive bedrock terrains, although these could be represented by either the Deccan Plateau flood basalts or the magmatic arc units in the Indus Suture Zone, including Kohistan. Because erosion is rapid and the sediment in the Indus River is relatively chemically fresh, as demonstrated by the overall low CIA, it seems more likely that strongly weathered, primitive material would be coming from the Deccan Plateau where chemical weathering has been impacting the landscape since the end of the eruption in the Paleocene (Widdowson & Cox 1996; Dessert *et al.* 2001).

Considering only the new data from this study (Fig. 9B), the same positive correlation is noted, but the correlation coefficient is substantially better, especially at Site U1456 ($R^2 = 0.56$ compared to 0.27). This result provides further support for the importance of using fine-grained samples for CIA-based weathering reconstructions. Nonetheless, this plot has to be interpreted with some caution because the Nd isotope data is from an earlier work (Clift *et al.* 2019) and the two datasets are not from the same samples. To be able to make any comparison, we must assume that analyses made on samples taken from close to the earlier Nd isotope measurements (<10 m) would have similar isotope character. This is reasonable because provenance changes slowly through time as the source ranges uplift. The improved correlation mirrors the temporal trend to lower CIA, which is particularly pronounced at Site U1456 compared to Site U1457. As well as reflecting varying input from the Deccan Plateau, some of the trend may be related to progressively faster erosion of old continental rocks uplifted in the Himalayas, which would reduce ε_{Nd} values while also decreasing the CIA.

7. Different sediment sources to different drilling sites

The new data presented here, together with a reassessment of the previously published data, now allows us to better explain why the chemical trend highlighted by Zhou *et al.* (2021) was so noisy. Part of this scatter is related to grain size. A larger range of grain sizes was used in the earlier record but results in the greater spread in values of various chemical weathering proxies such as CIA (Fig. 2). Because the sediment is not consistently fining or coarsening upsection, this means that there is variability introduced into the earlier record because of randomly analysing coarse or fine-grained material. This reinforces the need to use a uniform grain-size range when attempting to reconstruct palaeo-weathering conditions.

In the reconstruction presented above, it is also clear that sediment is coming into the Laxmi Basin from more than one source. One source is the Indus River, and the other is Peninsular India, largely dominated by the Deccan Plateau. Mixing calculations based on an average ε_{Nd} value of −2.4 for the Deccan Plateau and the evolving average for the Indus River (Clift *et al.* 2019) indicate that ~20–30% of the Upper Miocene at Site U1457 is from the Deccan Plateau, rising to 24–37% in the Pliocene and 31–35% in the Pleistocene. This is the other important factor causing a noisy record in the earlier study. Because the source compositions and weathering conditions are quite different in these two areas, mixing sediments derived from different regions results in a more random pattern than might be otherwise expected. In this work where we focus on muddy sediment, there is a relatively gradual and more orderly evolution in the intensity of chemical alteration of the sediment especially at Site U1456 and after 8 Ma (Fig. 8). As a result, two types of sedimentary systems can be recognized. One is finer grained and is derived from the Indus River. It shows decreasing degrees of chemical alteration through time and is preferentially deposited in the centre of the basin at Site U1456. The second system is slightly coarser grained

https://doi.org/10.1017/S0016756824000499 Published online by Cambridge University Press

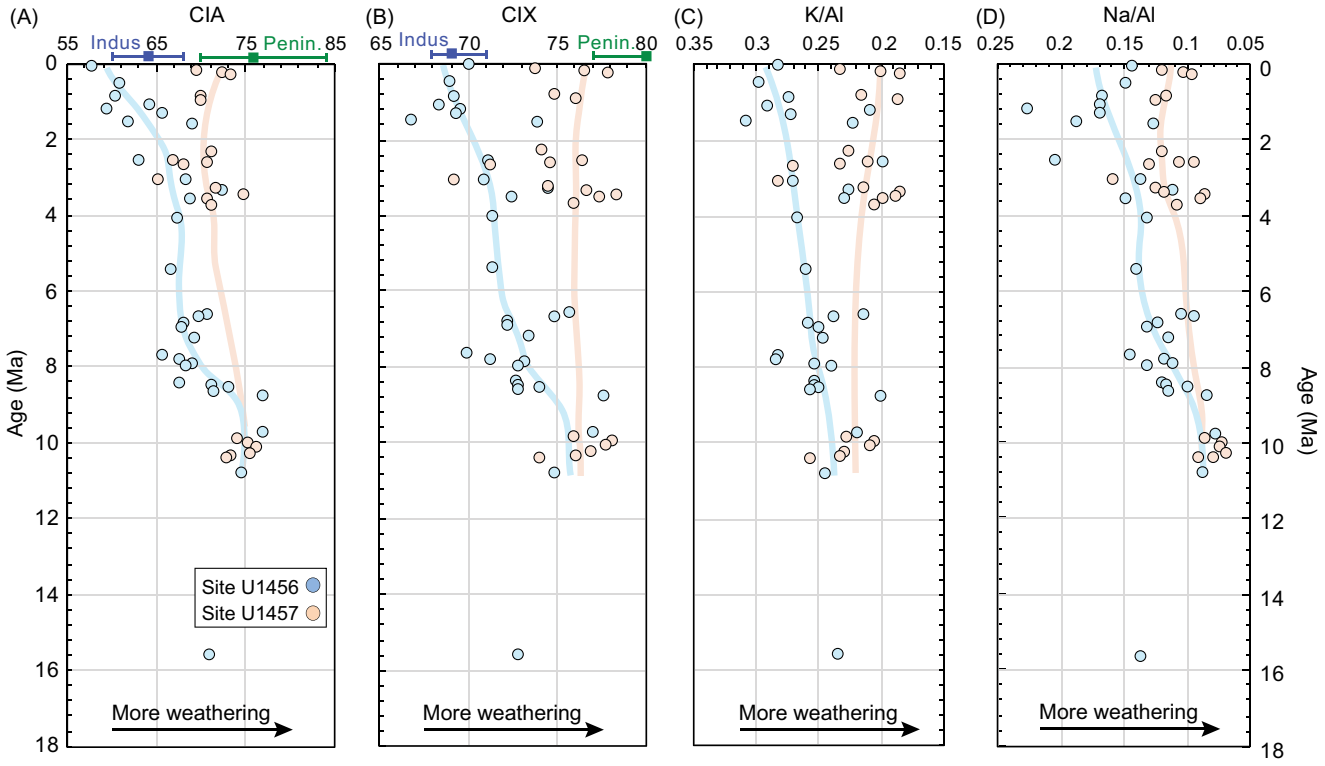

Figure 8. Temporal evolution in chemical weathering indices. (A) Chemical Index of Alteration (CIA) (Nesbitt *et al.* 1980), (B) CIA excluding Ca (CIX) (Garzanti *et al.* 2014), (C) K/Al and (D) Na/Al. Note diverging trends between Site U1456 (blue line) and U1457 (pink line), with Site U1456 sediment trending to less alteration with time but Site U1457 sediment remaining more constant.

and is derived from peninsular India. It is generally more strongly weathered and does not evolve much through time. Sediment from this source is deposited at both sites but is preferentially preserved at Site U1457. This is slightly surprising because Site U1457 is on the western side of Laxmi Basin, further from the Indian coast. Although aeolian dust is blown east from Arabia into the basin, the difference in transport distance between Sites U1456 and U1457 is not great, and earlier analysis of the isotopes has argued that influence from Arabian is insignificant (Clift *et al.* 2019). We infer that sediment coming from the north, from the Indus River mouth, is funnelled into the deepest axial part of the basin. Sediment coming from peninsular India must cross the basin in order to be deposited at Site U1457. We note that material from the peninsula is not exclusively found at Site U1457. Our reassessment of the provenance is consistent with the palynology data from Feakins *et al.* (2020), which focused on the older part of the section but also recognized the alternation of sediment supply from the north and from the east at Site U1457, albeit only in the Miocene.

8. Calculating CO_2 consumption

We use the new geochemical data to reassess the impact of chemical weathering in the Indus Basin on the consumption of carbon dioxide by the breakdown of silicate minerals. The Indus Basin represents a significant component of the Himalayan weathering budget that was proposed by Raymo and Ruddiman (1992) to have driven Cenozoic global cooling. In a recent synthesis, Clift *et al.* (2024b) suggested that the Indus Basin dominated the Asian carbon budget prior to the Late Miocene. The new dataset is focused on a limited grain-size variation more typical of the bulk volume of the submarine fan and has been more carefully decarbonated before analysis. By estimating the change in composition of sediment relative to fresh source bedrock, the amount of CO_2 consumed per unit weight can be estimated (France-Lanord & Derry 1997).

Changes in the molar ratios of Mg/Al, Ca/Al, Na/Al and K/Al are used to derive the ΔCO_2 values for each sample, that is, how much CO_2 is consumed per unit weight of sediment. We use the Nd isotopic data as interpreted by Clift *et al.* (2019) to determine if sediments were Indus River or peninsula-derived; however, because the isotope data come from samples analysed in a previous study rather than this one, we had to assume that sources did not change rapidly with time in order to assign our new data to an appropriate source, as explained above. After eliminating sediment eroded from the peninsula, we were able to estimate the composition of the evolving Indus River's bedrock sources following the existing model. This involves using the ε_{Nd} value to estimate the contributions from primitive sources within the Indus Suture Zone including the Karakoram (average ε_{Nd} value of -5 (Clift & Jonell 2021)), compared to older continental rocks in the Himalayas (average ε_{Nd} value of −15.7), and then using average crustal compositions from these areas to calculate an average source major element composition at any one particular time. The Himalayas are assumed to have an average UCC (Rudnick & Gao 2003), while Kohistan-Karakoram values are derived from the Georock database. The differences between the bedrock and the sediment Mg/Al, Ca/Al, Na/Al and K/Al values are then used to calculate the ΔCO_2 values using the method of France-Lanord and Derry (1997).

Some samples show a negative difference in K/Al values, which should be impossible because this implies that the sediment is less depleted than the bedrock source. This discrepancy is caused by

https://doi.org/10.1017/S0016756824000499 Published online by Cambridge University Press

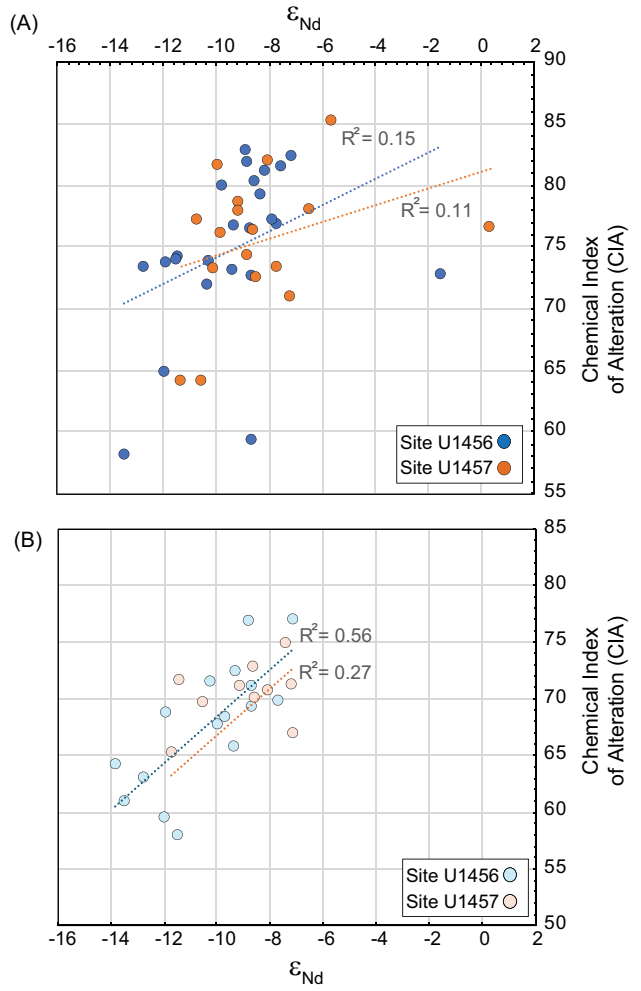

Figure 9. (A) Cross plot of Nd isotope composition against the Chemical Index of Alteration (CIA) for the data published by Zhou *et al.* (2021). (B) The same cross plot but with data from this study. Note the better correlation in the new study and the overall positive correlation between these two geochemical proxies.

reverse weathering, which is a process in which K is fixed into the deposited marine sediment in the form of diagenetic clay minerals, for example, smectite (Mackenzie & Kump 1995; Dunlea *et al.* 2017). This process is hard to correct accurately, although this is not a serious source of error because the amount of this negative difference is quite small and because K contributes a relatively moderate amount to the total CO_2 consumption. Its contribution is weighted as just 10% compared to the CO_2 consumption by Mg and Ca (France-Lanord & Derry 1997).

Figure 10A shows the results of the recalculation of the ΔCO_2 based on the new geochemical analyses. Our analysis shows that the ΔCO_2 values started at around 0.8–1.0 mol/y at 10 Ma and subsequently decreased to the present day, reaching ΔCO_2 values ~0.6–0.8 mol/y. This means that the amount of CO_2 consumed per unit weight of rock weathered decreased through time to the present. There is short-term variability related to changes in the sediment geochemistry, so a more representative long-term estimate may be derived using a five-point running average. The long-term changing chemical reactivity of rocks in the Indus Basin is linked to lower degrees of alteration and the reducing input from the more mafic rocks of the Karakoram, Kohistan and suture zone since ~8 Ma (Clift *et al.* 2019; Zhou *et al.* 2022). These rocks break down more readily and have a bigger impact of CO_2 consumption because of their high Mg contents.

We compare our estimates with the long-term estimates of ΔCO_2 values based on the Zhou *et al.* (2021) data and recently published by Clift *et al.* (2024b). Although the ΔCO_2 values were slightly higher according to Zhou *et al.* (2021) at 10 Ma, 1.0–1.2 mol/y (Fig. 10A), our new values were lower and showed a decrease from that time towards the present. In general, ΔCO_2 values were 1.0–0.8 mol/y and then dipped below 0.7 mol/y in the latter part of the Pleistocene. This means that the amount of CO_2 consumed per unit weight of sediment and thus the total CO_2 budget based on the earlier work yielded estimates of CO_2 consumption that are ~30% higher during the Miocene and ~60–70% in the Pleistocene than those based on data from this work. Given the large size of the Indus submarine fan and the prolific erosional flux from the Himalayas, this would result in a significant overestimate of the carbon sequestering power of chemical weathering in this region. In this case, it is less likely that chemical weathering in the Western Himalaya-Karakoram would be a critical factor in driving global cooling in the Plio-Pleistocene. This result emphasizes the importance of choosing appropriate material and undertaking rigorous carbonate removal prior to major element analysis if representative estimates of CO_2 sequestration are to be made over significant periods of geological time.

We infer that grain size is the more important of these factors distinguishing this and earlier work. Although finer grained, the sediments considered here were less altered than the sandier sediments analysed previously (Fig. 5). Sandy sediments are richer in quartz but depleted in minerals rich in Ca, Mg, K and Na that determine the amount of CO_2 consumed during weathering. In contrast, incomplete decarbonation would tend to result in elevated Ca contents and thus less CO_2 reduction, which is the opposite of what we see in these data. Total CO_2 consumption is more strongly controlled by the rates of sediment supply to the ocean rather than the degree of alteration (Clift *et al.* 2024b), and the temporal trends reconstructed for Asia are not greatly altered by this work, but the total amount of CO_2 consumed is reduced.

9. Conclusions

Calculating chemical weathering fluxes is critically dependent on accurate estimates of the average composition of sediments deposited in the depocentres of major drainage systems. While scientific drilling of the Indian Ocean submarine fans has provided samples of the largest depositional bodies on Earth, the resultant temporal histories of weathering history have yielded variable records often with poorly defined trends, especially when compared to hemipelagic sites. In this work, we assessed whether grain size or incomplete decarbonation prior to major element analysis might be affecting the results from the Indus submarine fan. We show that when fine-grained muddy sediments are preferentially selected and carefully decarbonated, the trends in chemical weathering intensity are more clearly defined. The data also highlight that sediments from the Laxmi Basin are derived from both the Indus River and Peninsular India. The former are in general less weathered than those eroded from the Craton or Deccan Plateau. Sediments deposited at Site U1456 are finer grained and preferentially more Indus River-derived than those at Site U1457. If these groups are treated separately, then a clear trend to less chemical alteration over time since ~8 Ma is visible in the Indus River.

https://doi.org/10.1017/S0016756824000499 Published online by Cambridge University Press

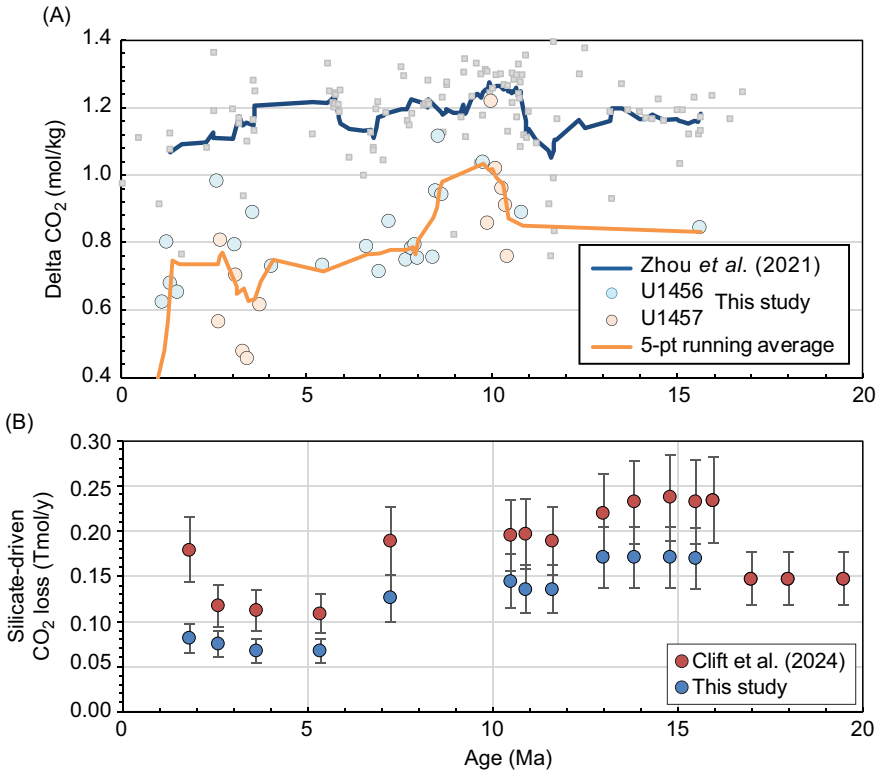

Figure 10. (A) Temporal evolution in the CO_2 consumption capacity of the Indus Fan sediments based on the new analyses compared with the estimates in Clift *et al.* (2024b) based on analyses from Zhou *et al.* (2021). ΔCO_2 is a measure of how much CO_2 is consumed per unit weight of sediment. (B) Total chemical weathering flux for the Indus Basin accounting for sedimentation rates after Clift (2006).

The major element composition of the Indus River-derived sediments can be used to recalculate the amount of CO_2 consumed per unit weight during chemical degradation. The value was moderately lower than earlier estimates at ~10 Ma but decreased over time, especially after ~8 Ma, so that in the recent geologic past, the estimates were ~60–70% lower than values based on earlier geochemical work. This result does not change the overall trend of CO_2 consumption in the Western Himalaya since the Middle Miocene, but it does reduce the total amount of CO_2 removed and further weakens arguments that Himalaya erosion and weathering drove Neogene global cooling.

Supplementary material. The supplementary material for this article can be found https://doi.org/10.1017/S0016756824000499.

Acknowledgements. We thank the Charles T. McCord Jr Chair in Petroleum Geology at Louisiana State University (LSU) for the financial support needed to undertake this study. We further thank Dr Matthew Loocke (LSU) for his help in undertaking the major element analysis and Ms. Wanda LeBlanc for her help and advice in sample preparation. The manuscript was improved by comments from two anonymous reviewers.

References

Andò S, Aharonovich S, Hahn A, George SC, Clift PD and Garzanti E (2020) Integrating heavy-mineral, geochemical and biomarker analyses of Plio-Pleistocene sandy and silty turbidites: a novel approach for provenance studies (Indus Fan, IODP Expedition 355). *Geological Magazine* **157**(6), 929–38, doi: 10.1017/S0016756819000773.

Anthony JW, Bideaux RA, Bladh KW and Nichols MC (2022) Ilmenite. In *Handbook of Mineralogy* Chantilly, VA, USA: Mineralogical Society of America.

Bayon G, Patriat M, Godderis Y, Trinquier A, De Deckker P, Kulhanek DK, Holbourn A and Rosenthal Y (2023) Accelerated mafic weathering in Southeast Asia linked to late Neogene cooling. *Science Advances* **9**(13), eadf3141, doi: 10.1126/sciadv.adf3141.

Berner RA and Berner EK (1997) Silicate weathering and climate. In *Tectonic Uplift and Climate Change* (ed WF Ruddiman). New York: Springer. 353–65.

Bouma AH (2001) Fine-grained submarine fans as possible recorders of long- and short-term climatic changes. *Global and Planetary Change* **28**(1), 85–91, doi: 10.1016/S0921-8181(00)00066-7.

Cai M, Xu Z, Clift PD, Khim BK, Lim D, Yu Z, Kulhanek DK and Li T (2020) Long-term history of sediment inputs to the eastern Arabian Sea and its implications for the evolution of the Indian summer monsoon since 3.7 Ma. *Geological Magazine* **157**(6), 908–19, doi: 10.1017/S0016756818000857.

Cai M, Xu Z, Clift PD, Lim D, Khim BK, Yu Z, Kulhanek DK and Li T, Chen H & Sun R (2019) Depositional History and Indian Summer Monsoon Controls on the Silicate Weathering of Sediment Transported to the Eastern Arabian Sea: Geochemical Records From IODP Site U1456 Since 3.8 Ma. *Geochemistry, Geophysics, Geosystems* **20**(9), 4336–53, doi: 10.1029/2018GC008157.

Carter SC., Griffith EM, Clift PD, Scher HD and Dellapenna TM (2020) Clay-fraction strontium and neodymium isotopes in the Indus Fan: implications for sediment transport and provenance. *Geological Magazine* **157**(6), 879–94, doi: 10.1017/S0016756820000394.

Caves Rugenstein JK, Ibarra, DE and von Blanckenburg F (2019) Neogene cooling driven by land surface reactivity rather than increased weathering fluxes. *Nature* **571**(7763), 99–102, doi: 10.1038/s41586-019-1332-y.

Clift PD (2006) Controls on the erosion of Cenozoic Asia and the flux of clastic sediment to the ocean. *Earth and Planetary Science Letters* **241**(3-4), 571–80, doi: 10.1016/j.epsl.2005.11.028.

Clift PD (2017) A revised budget for Cenozoic sedimentary carbon subduction. *Reviews of Geophysics* **55**, 97–125, doi: 10.1002/2016RG000531.

Clift PD, Du Y, Mohtadi M, Pahnke K, Sutorius M and Böning P (2024a) The Erosional and weathering response to arc-continent collision in New Guinea. *Journal of the Geological Society* **181**(4), doi: 10.1144/jgs2023-207.

Clift PD and Jonell TN (2021) Himalayan-Tibetan Erosion is not the Cause of Neogene Global Cooling. *Geophysical Research Letters* **48**(8), e2020GL087742, doi: 10.1029/2020GL087742.

Clift PD, Jonell TN, Du Y and Bornholdt T (2024b) The impact of Himalayan-Tibetan erosion on silicate weathering and organic carbon burial. *Chemical Geology* **656**, 122106, doi: 10.1016/j.chemgeo.2024.122106.

Clift PD, Shimizu N, Layne G, Gaedicke C, Schlüter HU, Clark MK and Amjad S (2001) Development of the Indus Fan and its significance for the erosional history of the western Himalaya and Karakoram. *Geological Society of America Bulletin* **113**, 1039–51, doi: 10.1130/0016-7606(2001)113<1039:DOTIFA>2.0.CO;2.

Clift PD, Zhou P, Stockli DF and Blusztajn J (2019) Regional Pliocene exhumation of the Lesser Himalaya in the Indus drainage. *Solid Earth* **10**, 647–61, doi: 10.5194/se-10-647-2019.

Dailey SK, Clift PD, Kulhanek DK, Blusztajn J, Routledge CM, Calvès G, O'Sullivan P, Jonell TN, Pandey DK, Andò S, Coletti G, Zhou P, Li Y, Neubeck NE, Bendle JAP, Bratenkov S, Griffith EM, Gurumurthy GP, Hahn A, Iwai M, Khim BK, Kumar A, Kumar AG, Liddy HM, Lu H, Lyle MW, Mishra R, Radhakrishna T, Saraswat R, Saxena R, Scardia G, Sharma GK, Singh AD, Steinke S, Suzuki K, Tauxe L, Tiwari M, Xu Z and Yu Z (2019) Large-scale mass wasting on the Miocene Continental Margin of Western India. *Geological Society of America Bulletin* **132**(1-2), 85–112, doi: 10.1130/B35158.1.

Dawson JB and Smith JV (1975) 26 - Chromite-silicate intergrowths in upper mantle peridotites. In *Physics and Chemistry of the Earth* (eds LH Ahrens, JB Dawson, AR Duncan and AJ Erlank), pp. 339–50 Pergamon., doi: 10.1016/B978-0-08-018017-5.50030-4.

Dessert C, Dupré B, Francois LM, Schott J, Gaillardet J, Chakrapani G and Bajpai S (2001) Erosion of Deccan Traps determined by river geochemistry: impact on the global climate and the 87Sr/86Sr ratio of seawater. *Earth and Planetary Science Letters* **188**, 459–74.

Droz L and Bellaiche G (1991) Seismic facies and geologic evolution of the central portion of the Indus Fan. In *Seismic facies and sedimentary processes of submarine fans and turbidite systems* (eds P. Weimer and M. H. Link). pp. 383–402. Berlin: Springer Verlag.

Dunlea AG, Murray RW, Santiago Ramos DP and Higgins JA (2017) Cenozoic global cooling and increased seawater Mg/Ca via reduced reverse weathering. *Nature Communications* **8**(1), 844, doi: 10.1038/s41467-017-00853-5.

Exnicios EM, Carter A, Najman Y & Clift P.D. (2022) Late Miocene unroofing of the Inner Lesser Himalaya recorded in the NW Himalaya foreland basin. *Basin Research* **34**(6), 1894–916, doi: 10.1111/bre.12689.

Feakins SJ, Liddy HM, Tauxe L, Galy V, Feng X, Tierney JE, Miao Y and Warny S (2020) Miocene C4 Grassland Expansion as Recorded by the Indus Fan. *Paleoceanography and Paleoclimatology* **35**(6), e2020PA003856, doi: 10.1029/2020PA003856.

Fedo CM, Nesbitt HW and Young GM (1995) Unraveling the effects of potassium metasomatism in sedimentary rocks and paleosols, with implications for paleoweathering conditions and provenance. *Geology* **23**, 921–24.

Folk RL (1974.) Petrology of Sedimentary Rocks. Austin, Texas: Hemphill Press.

France-Lanord C and Derry LA (1997) Organic carbon burial forcing of the carbon cycle from Himalayan erosion. *Nature* **390**, 65–67.

Garzanti E, Andò S and Vezzoli G (2020) Provenance of Cenozoic Indus Fan Sediments (IODP Sites U1456 and U1457). *Journal of Sedimentary Research* **90**(9), 1114–27, doi: 10.2110/jsr.2019-195.

Garzanti E, Vermeesch P, Padoan M, Resentini A, Vezzoli G and Andò S (2014) Provenance of Passive-Margin Sand (Southern Africa). *The Journal of Geology* **122**(1), 17–42, doi: 10.1086/674803.

Garzanti E, Vezzoli G, Andò S, Paparella P and Clift PD (2005) Petrology of Indus River sands; a key to interpret erosion history of the western Himalayan syntaxis. *Earth and Planetary Science Letters* **229**(3-4), 287–302, DOI: 10.1016/j.epsl.2004.11.008.

Goldstein, SL, O'Nions, RK and Hamilton, PJ (1984) A Sm-Nd isotopic study of atmospheric dusts and particulates from major river systems. *Earth and Planetary Science Letters* **70**(2), 221–36.

He M, Zheng H, Clift, PD, Tada R, Wu W and Luo C (2015) Geochemistry of fine-grained sediments in the Yangtze River and the implications for provenance and chemical weathering in East Asia. *Progress in Earth and Planetary Science* **2**(32), 1–20, doi: 10.1186/s40645-015-0061-6.

Hodges KV (2000) Tectonics of the Himalaya and southern Tibet from two perspectives. *Geological Society of America Bulletin* **112**(3), 324–50.

Hülse P and Bentley SJ (2012) A 210Pb sediment budget and granulometric record of sediment fluxes in a subarctic deltaic system: The Great Whale River, Canada. *Estuarine, Coastal and Shelf Science* **109**, 41–52, doi: 10.1016/j.ecss.2012.05.019.

Jagoutz O, Müntener O, Ulmer P, Pettke T, Burg JP, Dawood H and Hussain S (2007) Petrology and mineral chemistry of lower crustal intrusions: the Chilas Complex, Kohistan (NW Pakistan). *Journal of Petrology* **48** (10), 1895–953, doi: 10.1093/petrology/egm044.

Kelemen PB and Manning CE (2015) Reevaluating carbon fluxes in subduction zones, what goes down, mostly comes up. *Proceedings of the National Academy of Sciences* **112**(30), E3997–E4006, doi: 10.1073/pnas.1507889112.

Kessarkar PM, Purnachandra RV, Ahmad SM and Babu GA (2003) Clay minerals and Sr-Nd isotopes of the sediments along the western margin of India and their implication for sediment provenance. *Marine Geology* **202**(1-2), 55–69, doi: 10.1016/S0025-3227(03)00240-8.

Khan MA, Stern RJ, Gribble RF and Windley BF (1997) Geochemical and isotopic constraints on subduction polarity, magma sources, and palaeogeography of the Kohistan intra-oceanic arc, northern Pakistan Himalaya. *Journal of the Geological Society, London* **154**, 935–46.

Kolla V and Coumes F (1991) Seismic stratigraphy, canyon and channel characteristics of the Indus continental margin and upper fan. In *Seismic facies and sedimentary processes of submarine fans and turbidite systems* (eds P. Weimer and M. H. Link),p. 438 Berlin: Springer Verlag.

Kump LR and Arthur MA (1997) Global chemical erosion during the Cenozoic: weatherability balances the budget. In *Tectonics, Uplift and Climate Change* (ed WF Ruddiman), pp. 399–426. New York: Plenum Publishing Co.,

Kurian S, Nath BN, Kumar NC and Nair KKC (2013) Geochemical and isotopic signatures of surficial sediments from the Western continental shelf of India: inferring provenance, weathering, and the nature of organic matter geochemical and isotopic signatures of sediments from the Indian West Coast. *Journal of Sedimentary Research* **83**(6), 427–42, doi: 10.2110/jsr.2013.36.

Limmer DR, Boening P, Giosan L, Ponton C, Köhler, CM, Cooper, MJ, Tabrez, AR and Clift PD (2012) Geochemical record of Holocene to recent sedimentation on the Western Indus continental shelf, Arabian Sea. *Geochemistry Geophysics Geosystems* **13**(Q01008), doi: 10.1029/2011GC003845.

Lorand JP & Ceuleneer G (1989) Silicate and base-metal sulfide inclusions in chromites from the Maqsad area (Oman ophiolite, Gulf of Oman): A model for entrapment. *Lithos* **22**(3), 173–90, doi: 10.1016/0024-4937(89)90054-6.

Mackenzie FT and Kump LR (1995) Reverse weathering, clay mineral formation, and oceanic element cycles. *Science* **270**(5236), 586–87, doi: 10.1126/science.270.5236.586.

Martin PE, Macdonald FA, McQuarrie N, Flowers RM and Maffre PJY (2023) The rise of New Guinea and the fall of Neogene global temperatures. *Proceedings of the National Academy of Sciences* **120**(40), e2306492120, doi: 10.1073/pnas.2306492120.

McHargue TR & Webb JE (1986) Internal geometry, seismic facies, and petroleum potential of canyons and inner fan channels of the Indus submarine fan. *AAPG Bulletin* **70**, 161–80.

Miles PR, Munschy M and Ségoufin J (1998) Structure and early evolution of the Arabian Sea and east Somali Basin. *Geophysical Journal International* **134**, 876–888. doi: 10.1046/j.1365-246x.1998.00625.x.

Naini BR and Kolla V (1982) Acoustic character and thickness of sediments of the Indus Fan and the continental margin of western India. *Marine Geology* **47**, 181–95.

Najman Y, Bickle M, Garzanti E, Pringle M, Barfod D, Brozovic N, Burbank D and Ando S (2009) Reconstructing the exhumation history of the Lesser Himalaya, NW India, from a multitechnique provenance study of the foreland basin Siwalik Group. *Tectonics* **28**,TC5018, doi: 10.1029/2009TC002506.

Nesbitt HW, Markovics G and Price RC (1980) Chemical processes affecting alkalis and alkaline earths during continental weathering. *Geochimica et Cosmochimica Acta* **44**, 1659–66.

Nesbitt HW and Young GM (1982) Early Proterozoic climates and plate motions inferred from major element chemistry of lutites. *Nature* **299**(5885), 715–17.

Pandey DK, Clift PD, Kulhanek DK, Andò S, Bendle JAP, Bratenkov S, Griffith EM, Gurumurthy GP, Hahn A, Iwai M, Khim, B-K, Kumar A, Kumar A G, Liddy HM, Lu H, Lyle MW, Mishra R, Radhakrishna T, Routledge CM, Saraswat R, Saxena R, Scardia G, Sharma GK, Singh AD,

https://doi.org/10.1017/S0016756824000499 Published online by Cambridge University Press

Steinke S, Suzuki K, Tauxe L, Tiwari M, Xu Z and Yu Z (2016a) Site U1456. *Proceedings of the International Ocean Discovery Program* 355, doi:10.14379/iodp.proc.355.103.2016.

Pandey DK, Clift PD, Kulhanek DK, Andò S, Bendle JAP, Bratenkov S, Griffith EM, Gurumurthy GP, Hahn A, Iwai M, Khim BK, Kumar A, Kumar A G, Liddy HM, Lu H, Lyle MW, Mishra R, Radhakrishna T, Routledge CM, Saraswat R, Saxena R, Scardia G, Sharma GK, Singh AD, Steinke S, Suzuki K, Tauxe L, Tiwari M, Xu Z and Yu Z (2016b) Site U1457. *Proceedings of the International Ocean Discovery Program* 355, doi: 10.14379/iodp.proc.355.104.2016.

Pandey DK, Clift, PD, Kulhanek DK and Expedition 355 Scientists (2016c) Arabian Sea Monsoon. *Proceedings of the International Ocean Discovery Program* 355, doi: 10.14379/iodp.proc.355.2016.

Pandey DK, Pandey A, Clift PD, Nair N, Ramesh P, Kulhanek DK and Yadav R (2020) Flexural subsidence analysis of the Laxmi Basin, Arabian Sea and its tectonic implications. *Geological Magazine* **157**, 834–47, doi: 10.1017/S0016756818000833.

Raymo ME and Ruddiman WF (1992) Tectonic forcing of Late Cenozoic climate. *Nature* **359**(6391), 117–22, doi: 10.1038/359117a0.

Routledge CM, Kulhanek DK, Tauxe L, Scardia G, Singh AD, Steinke S, Griffith EM & Saraswat R (2020) Revised geological timescale for IODP Sites U1456 and U1457. *Geological Magazine* **157**(6), 961–78, doi: 10.1017/S0016756819000104.

Rudnick RL and Gao S (2003) The composition of the continental crust. In *The Crust* (ed R. L. Rudnick). Oxford: Elsevier-Pergamon. Treatise on Geochemistry, 3, 1–64.

Searle MP, Rex AJ, Tirrul R, Rex DC, Barnicoat A and Windley BF (1989) Metamorphic, magmatic and tectonic evolution of the Central Karakoram in the Biafo-Baltoro-Hushe regions of north Pakistan. *Geological Society of America Special Paper* **232**, 47–73.

Singh M, Sharma M and Tobschall HJ (2005) Weathering of the Ganga alluvial plain, northern India: implications from fluvial geochemistry of the Gomati River. *Applied Geochemistry* **20**, 1–21, doi: 10.1016/j.apgeochem.2004.07.005.

Stow DAV, Howell DG and Nelson CH (1985) Sedimentary, Tectonic, and Sea-Level Controls. In *Submarine Fans and Related Turbidite Systems* (eds A. H. Bouma, W. R. Normark and N. E. Barnes). New York, NY: Springer New York. 15–22, doi: 10.1007/978-1-4612-5114-9_4.

Sundell K and Saylor JE (2017) Unmixing detrital geochronology age distributions. *Geochemistry Geophysics Geosystems* **18**, 2872–86.

Tachambalath AP, France-Lanord C, Galy A, Rigaudier T and Charreau J (2023) Data report: major and trace element composition of silicates and carbonates from Bengal Fan sediments, IODP Expedition 354. *Proceedings of the International Ocean Discovery Program* **354**, 1–10, doi: 10.14379/iodp.proc.354.204.2023.

Talwani M and Reif C (1998) Laxmi Ridge - A continental sliver in the Arabian Sea. *Marine Geophysical Researches* **20**, 259–71.

Taylor SR and McLennan SM (1995) The geochemical evolution of the continental crust. *Reviews of Geophysics* **33**, 241–65.

West AJ, Galy A and Bickle MJ (2005) Tectonic and climatic controls on silicate weathering. *Earth and Planetary Science Letters* **235**, 211–28, doi: 10.1016/j.epsl.2005.03.020.

Westerhold T, Marwan N, Drury AJ, Liebrand D, Agnini C, Anagnostou E, Barnet JSK, Bohaty SM, De Vleeschouwer D, Florindo F, Frederichs T, Hodell DA, Holbourn AE, Kroon D, Lauretano V, Littler K, Lourens LJ, Lyle M, Pälike H, Röhl U, Tian J, Wilkens RH, Wilson PA and Zachos JC (2020) An astronomically dated record of Earth's climate and its predictability over the last 66 million years. *Science* **369**(6509), 1383–87, doi: 10.1126/science.aba6853.

Widdowson M and Cox KG (1996) Uplift and erosional history of the Deccan Traps, India: evidence from laterites and drainage patterns of the Western Ghats and Konkan Coast. *Earth and Planetary Science Letters* **137**, 57–69.

Yu Z, Colin C, Wan S, Saraswat R, Song L, Xu Z, Clift P, Lu H, Lyle M, Kulhanek D, Hahn A, Tiwari M, Mishra R, Miska S and Kumar A (2019) Sea level-controlled sediment transport to the eastern Arabian Sea over the past 600 kyr: clay minerals and SrNd isotopic evidence from IODP site U1457. *Quaternary Science Reviews* **205**, 22–34, doi: 10.1016/j.quascirev.2018.12.006.

Zack T and Kooijman E (2017) Petrology and geochronology of rutile. *Reviews in Mineralogy and Geochemistry* **83**(1), 443–67, doi: 10.2138/rmg.2017.83.14.

Zhou P, Carter A, Li Y and Clift PD (2020) Slowing rates of regional exhumation in the Western Himalaya: fission track evidence from the Indus Fan. *Geological Magazine* **157**, 848–63, doi: 10.1017/S0016756819000608.

Zhou P, Ireland T, Murray RW and Clift PD (2021) Marine sedimentary records of chemical weathering evolution in the Western Himalaya since 17 Ma. *Geosphere* **17**(3), 824–53, doi: 10.1130/GES02211.1.

Zhou P, Stockli DF, Ireland T, Murray RW and Clift PD (2022) Zircon U-Pb age constraints on NW Himalayan exhumation from the Laxmi Basin, Arabian Sea. *Geochemistry, Geophysics, Geosystems* **23**(1), e2021GC010158, doi: 10.1029/2021GC010158.